All-optical generation of Brillouin dynamic grating based on multiple acoustic modes in a single-mode dispersion-shifted fiber

Weiwen Zou* **and Jianping Chen**

State Key Laboratory of Advanced Optical Communication Systems and Networks, Department of Electronic Engineering, Shanghai Jiao Tong University, Shanghai 200240, China
wzou@sjtu.edu.cn

Abstract: We demonstrate an all-optical generation of Brillouin dynamic grating (BDG) in a single-mode dispersion-shifted fiber (DSF). The feature of multiple-peak Brillouin gain spectrum (BGS) owing to the existence of the multiple acoustic modes in the single-mode DSF is utilized. Two inharmonic lock-in detections are newly introduced to characterize the BGS and the frequency-maintained or frequency-shifted BDG reflection. The frequency-shifted property of the BDG in the DSF with hundreds of MHz can find great potential applications in optical fiber sensing or all-optical signal processing.

OCIS codes: (290.5900) Scattering, stimulated Brillouin; (120.5820) Scattering measurements; (050.1950) Diffraction gratings; (060.2370) Fiber optics sensors.

References and links

1. K. Y. Song, W. Zou, Z. He, and K. Hotate, "All-optical dynamic grating generation based on Brillouin scattering in polarization-maintaining fiber," Opt. Lett. **33**(9), 926–928 (2008).
2. W. Zou, Z. He, and K. Hotate, "Complete discrimination of strain and temperature using Brillouin frequency shift and birefringence in a polarization-maintaining fiber," Opt. Express **17**(3), 1248–1255 (2009).
3. Y. Dong, L. Chen, and X. Bao, "Truly distributed birefringence measurement of polarization-maintaining fibers based on transient Brillouin grating," Opt. Lett. **35**(2), 193–195 (2010).
4. W. Zou, Z. He, and K. Hotate, "Demonstration of Brillouin distributed discrimination of strain and temperature using a polarization-maintaining optical fiber," IEEE Photon. Technol. Lett. **22**(8), 526–528 (2010).
5. W. Zou, Z. He, and K. Hotate, "One-laser-based generation/detection of Brillouin dynamic grating and its application to distributed discrimination of strain and temperature," Opt. Express **19**(3), 2363–2370 (2011).
6. Y. Dong, L. Chen, and X. Bao, "High-spatial-resolution time-domain simultaneous strain and temperature sensor using Brillouin scattering and birefringence in a polarization-maintaining fiber," IEEE Photon. Technol. Lett. **22**(18), 1364–1366 (2010).
7. K. Y. Song, S. Chin, N. Primerov, and L. Thévenaz, "Time-domain distributed fiber sensor with 1 cm spatial resolution based on Brillouin dynamic grating," J. Lightwave Technol. **28**(14), 2062–2067 (2010).
8. K. Y. Song, K. Lee, and S. B. Lee, "Tunable optical delays based on Brillouin dynamic grating in optical fibers," Opt. Express **17**(12), 10344–10349 (2009).
9. J. Sancho, N. Primerov, S. Chin, Y. Antman, A. Zadok, S. Sales, and L. Thévenaz, "Tunable and reconfigurable multi-tap microwave photonic filter based on dynamic Brillouin gratings in fibers," Opt. Express **20**(6), 6157–6162 (2012).
10. G. P. Agrawal, *Nonlinear Fiber Optics*, 4th ed. (Academic Press, 2007).
11. S. Afshar V, G. A. Ferrier, X. Bao, and L. Chen, "Effect of the finite extinction ratio of an electro-optic modulator on the performance of distributed probe-pump Brillouin sensor systems," Opt. Lett. **28**(16), 1418–1420 (2003).
12. D. P. Zhou, L. Chen, and X. Bao, "Polarization-decoupled four-wave mixing based on stimulated Brillouin scattering in a polarization-maintaining fiber," J. Opt. Soc. Am. B **30**(4), 821–828 (2013).
13. K. Y. Song, "Operation of Brillouin dynamic grating in single-mode optical fibers," Opt. Lett. **36**(23), 4686–4688 (2011).
14. S. Li, M. J. Li, and R. S. Vodhanel, "All-optical Brillouin dynamic grating generation in few-mode optical fiber," Opt. Lett. **37**(22), 4660–4662 (2012).
15. C. C. Lee, P. W. Chiang, and S. Chi, "Utilization of a dispersion-shifted fiber for simultaneous measurement of distributed strain and temperature through Brillouin frequency shift," IEEE Photon. Technol. Lett. **13**(10), 1094–1096 (2001).

#189904 - $15.00 USD Received 7 May 2013; revised 10 Jun 2013; accepted 10 Jun 2013; published 13 Jun 2013

16. Y. Koyamada, S. Sato, S. Nakamura, H. Sotobayashi, and W. Chujo, "Simulating and designing Brillouin gain spectrum in single-mode fibers," J. Lightwave Technol. **22**(2), 631–639 (2004).
17. A. Kobyakov, S. Kumar, D. Q. Chowdhury, A. B. Ruffin, M. Sauer, S. R. Bickham, and R. Mishra, "Design concept for optical fibers with enhanced SBS threshold," Opt. Express **13**(14), 5338–5346 (2005).
18. W. Zou, Z. He, and K. Hotate, "Acoustic modal analysis and control in w-shaped triple-layer optical fibers with highly-germanium-doped core and F-doped inner cladding," Opt. Express **16**(14), 10006–10017 (2008).
19. Y. Mizuno, W. Zou, Z. He, and K. Hotate, "Proposal of Brillouin optical correlation-domain reflectometry (BOCDR)," Opt. Express **16**(16), 12148–12153 (2008).
20. V. P. Kalosha, W. Li, F. Wang, L. Chen, and X. Bao, "Frequency-shifted light storage via stimulated Brillouin scattering in optical fibers," Opt. Lett. **33**(23), 2848–2850 (2008).
21. Z. Zhu, D. J. Gauthier, and R. W. Boyd, "Stored light in an optical fiber via stimulated Brillouin scattering," Science **318**(5857), 1748–1750 (2007).

1. Introduction

Recently, stimulated Brillouin scattering (SBS)in optical fibers has been proved to be a powerful way to generate Brillouin dynamic grating (BDG), which has attracted extensive interest in the fields of optical fiber sensing, microwave photonics, and all-optical signal processing [1–9].In fact, the concept of BDG was inspired by the nature of SBS [1, 10]. In the SBS process a longitudinal acoustic wave served as a dynamic grating can be optically generated via the elasto-optical effect as long as two counter-propagating optical waves (called pump and probe waves) have a precise frequency offset equal to the Brillouin frequency shift (BFS) [10]. The first demonstration of BDG was reported in a polarization-maintaining fiber (PMF) [1], where pump and probe waves generating or writing the BDG are launched along one of the principal polarization axis while the third read wave is injected along the other principal polarization axis. Strong diffraction of the read wave occurs only when the frequency difference between the pump and read waves is equal to the birefringence-determined phase-matching condition [1, 2].Consequently, the BDG provides an additional degree of freedom to precisely characterize the birefringence [2, 3], which has been shown to be an effective method to completely discriminate strain and temperature responses for Brillouin-based distributed optical fiber sensing applications [2–6]. The BDG in PMF was also used to realize high-spatial-resolution Brillouin optical time domain analysis (BOTDA) [7].It is advantageous over the pre-excited BOTDA firstly proposed in single-mode optical fibers (SMFs) [11] because the orthogonal feature between the writing and reading process of BDG separates efficiently the diffraction of the BDG from the pre-excited SBS. Besides, the BDG generation in PMF has been utilized as tunable delay line [8] or photonic microwave filter [9].A strict theoretical study [12] has verified that the essential aspect of the BDG in PMF is the polarization-decoupled four-wave mixing among the writing and reading optical waves assisted by the excited acoustic grating (i.e., BDG). Most recently, two other BDG generations were proposed in a SMF [13] or a few-mode optical fiber [14].

In this paper, we demonstrate an all-optical generation of BDG in a single-mode dispersion-shifted fiber (DSF). In a DSF, the SBS process can generate several acoustic modes, which induce a multiple-peak Brillouin gain spectrum (BGS) with well separated resonance frequencies of $\nu^{(i)}$ where the subscript "i" corresponds to the ith-order acoustic mode [15].Compared with the so-far BDG generation in a PMF [1], SMF [13] or few-mode optical fiber (FMF) [14],the BDG in a DSF can offer more interesting features. When the same fundamental acoustic mode is used for generation and detection of the BDG in a DSF, frequency-maintained reflection is obtained. Besides, when the fundamental acoustic mode is used for generation while a higher-order acoustic mode is used for detection, hundreds-of-MHz frequency-shifted reflection is achieved.

2. Principle

Figure 1(a) illustrates the principle of all-optical generation of BDG in optical fibers via the SBS process. Two coherent optical waves, i.e., the pump and probe (Stokes) waves in the SBS process, are launched from the two opposite ends of optical fibers. When their optical

#189904 - $15.00 USD Received 7 May 2013; revised 10 Jun 2013; accepted 10 Jun 2013; published 13 Jun 2013

frequency offset ($\nu_1 = f_1 - f_1'$) is equal to the Brillouin frequency shift (BFS,ν_B) as well as the resonance frequency of the fundamental acoustic mode ($\nu^{(1)}$):

$$\nu_1 \equiv f_1 - f_1' = \nu_B = \nu^{(1)}, \tag{1}$$

where f_1 and f_1' are the optical frequencies of the pump and probe waves, a strong acoustic wave of the fundamental acoustic mode (the so-called BDG) is optically generated. As long as the third optical wave (i.e., the read wave) is injected from the same end as the launching of the pump wave, there is a diffracted/reflected optical wave originating from the BDG. The diffraction or reflection efficiency (also called BDG reflectivity) is determined by the phase-matching condition, under which the pump/probe and read wave [1, 2, 13, 14] can efficiently couple their energy via the BDG [12].Up to date, the principle of BDG generation and detection can be classified into two different cases, which are dependent on the used optical fibers as schematically shown in Figs. 1(b) and 1(c), respectively.

In a PMF or FMF [see Fig. 1(b)], the BDG generation is separated from the BDG detection by use of orthogonal polarization states [1, 2] or different optical modes [14]. Its phase-matching condition means that the BDG generation and detection should share the unique BFS of the ν_B:

$$\nu_1^{(1)} = \nu_2^{(1)} = \nu_B, \tag{2}$$

where $\nu_1^{(1)}$ or $\nu_2^{(1)}$ is the BFS in the BDG generation or detection in optical fibers. They can be tuned by changing the optical frequencies of the pump and read waves:

$$\nu_1^{(1)} = \frac{2n_1}{c} \cdot V_a^{(1)} \cdot f_1, \tag{3}$$

$$\nu_2^{(1)} = \frac{2n_2}{c} \cdot V_a^{(1)} \cdot f_2, \tag{4}$$

where c is the optical velocity in vacuum, $V_a^{(1)}$ is the acoustic velocity of the fundamental acoustic wave, and f_2 is the optical frequency of the read wave.$n_1$and n_2 are the effective refractive indices of the pump and read wave, which are dependent on the polarization states of a PMF or the optical modes of a FMF. Consequently, the read and pump wave (as well as the BDG reflection and the SBS amplified probe) suffers a frequency difference according to Eqs. (2)-(4), which provides a very powerful way to monitor the birefringence change in a PMF [2, 12] or the relative change of the effective refractive indices in a FMF [14].

In this work, we propose a novel method to generate and detect BDG in a DSF, which can be generalized into the second case as depicted in Fig. 1(c). Again, the generation of BDG is occurred during the SBS process between the two coherent pump and probe wave with a precise optical frequency offset of ν_1 determined by Eq. (3). If the read wave with the optical frequency of f_2 is launched for BDG detection, multiple-peak Stokes wave is intrinsically backscattered via spontaneous Brillouin scattering. The *i*th-peak Stokes wave is downshifted in frequency from the read wave by

$$\nu_2^{(i)} = \frac{2n}{c} \cdot V_a^{(i)} \cdot f_2, \tag{5}$$

Where n = 1.448is the effective refractive index of the DSF with no difference between the BDG generation and detection due to the polarization-degenerate nature of the DSF, and $V_a^{(i)}$ is the acoustic velocity of the *i*th-order acoustic wave.

#189904 - $15.00 USD Received 7 May 2013; revised 10 Jun 2013; accepted 10 Jun 2013; published 13 Jun 2013

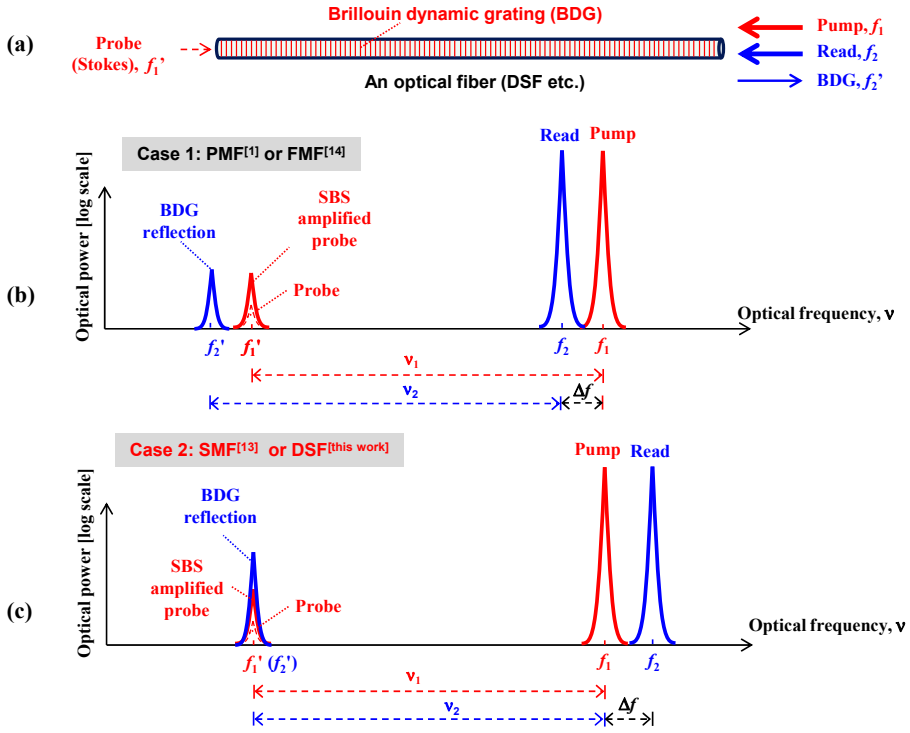

Fig. 1. Principle of BDG in DSF. (a): Orientation of optical injection. (b) and (c): Two different cases of the optical frequency relation among the pump, probe (Stokes), read, and BDG reflection.

When the *i*th-peak backscattered Stokes (or called BDG reflection) has the same optical frequency with the probe wave in the BDG generation, meaning

$$f_2 - \nu_2^{(i)} = f_1 - \nu_1^{(1)}, \tag{6}$$

four optical waves of the pump, probe, read and the BDG reflection (or Stokes) couple with each other via the BDG. By substituting Eqs. (3) and (5) into Eq. (6), one gets

$$\Delta f \equiv f_2 - f_1 = \frac{\nu_1^{(i)} - \nu_1^{(1)}}{1 - 2n \cdot V_a^{(i)} / c}, \tag{7}$$

where Δf is the optical frequency difference between the read and pump wave. $\nu_1^{(i)}$ is the *i*th-order resonance frequency of the BGS measured by the pump-probe SBS process, which is also given by Eq. (5) except that f_2 is replaced by f_1.The acoustic velocity ($V_a^{(i)}$ = ~5300-5900 m/s) in silica fibers is far smaller than the optical velocity (c = 3.0 × 10^8 m/s) [16], and the one in the used DSF will be experimentally demonstrated below. Hence, Eq. (6) can be approximately simplified as

$$\Delta f \cong \nu_1^{(i)} - \nu_1^{(1)}, \tag{8}$$

The energy coupling efficiency among the four optical waves or the BDG reflectivity of the read wave is proportional to the fact given by

$$\xi_{BDG} = \frac{A_{eff}^{ao(1)}}{A_{eff}^{ao(i)}}, \tag{9}$$

#189904 - $15.00 USD Received 7 May 2013; revised 10 Jun 2013; accepted 10 Jun 2013; published 13 Jun 2013

where $A_{eff}^{ao(1)}$ is the acousto-optic effective area between the optical mode and the fundamental acoustic wave, corresponding to the BDG generation via the pump-probe SBS process; and $A_{eff}^{ao(i)}$ denotes the *i*th-order acousto-optic effective area, determining the power of the *i*th-peak backscattered Stokes wave in the BDG detection. Both two areas are related to the fiber materials and optical/acoustic waveguide structure [17].

It is noted that the BDG recently observed in a SMF [13] can be regarded as one special example of the generalized second case with $f_2 = f_1$ and $\zeta_{BDG} = 1$ because the BDG generation and detection share the same fundamental acoustic mode.

3. Experimental details

3.1. Experimental setup

The experimental setup of characterizing BDG in a single-mode DSF (Furukawa)with 200-m length is depicted in Fig. 1. Two distributed feedback laser diodes (DFB-LD-1 and DFB-LD-2) work as the laser sources of BDG generation and detection, respectively. The output of the DFB-LD-1 is divided into two equal parts by a 3-dB coupler. One part is modulated by a single sideband modulator (SSBM) to generate frequency-downshifted Brillouin probe wave, which is amplified by an erbium-doped fiber amplifier (EDFA1) before launching into the DSF through an isolator (ISO1). The other part served as the Brillouin pump wave is chopped by an intensity modulator (IM1), amplified by an EDFA2, and injected into a circulator (CIR1).

The DFB-LD-2 is ramp-swept or detuned in frequency by a saw-tooth current generator, which is also chopped by an IM2 and amplified by an EDFA3. The ramp-swept light served as the BDG read wave goes through a CIR2 and combines with the Brillouin pump wave by a 3-dB coupler. One output of the coupler is detected by a power meter (PM) to monitor the optical power of the pump or read wave; the other is launched into the DSF. The polarization states of all three waves (pump, probe and read) are optimized by three polarization controllers (PCs) in each arm. The 3rd-port output of the CIR1 is measured by an optical spectrum analyzer (OSA) with a resolution of 0.01 nm; the one of the CIR2 is electrically detected and recorded after passing through a variable optical attenuator (VOA), a photo-detector (PD),a lock-in amplifier (LIA1 or LIA2), a data acquisition card (DAQ) and a computer. It is worth mentioning that the read wave has very close frequency to the pump wave according to Eq. (8), and it is very hard to separate each other by use of an optical filtering method [2].Hence, two individual LIA1 and LIA2, which are synchronized with the inharmonic chopping frequencies to the IM1 and IM2, are used to measure the BGS in the BDG generation and measure the BDG reflection, respectively.

#189904 - $15.00 USD Received 7 May 2013; revised 10 Jun 2013; accepted 10 Jun 2013; published 13 Jun 2013

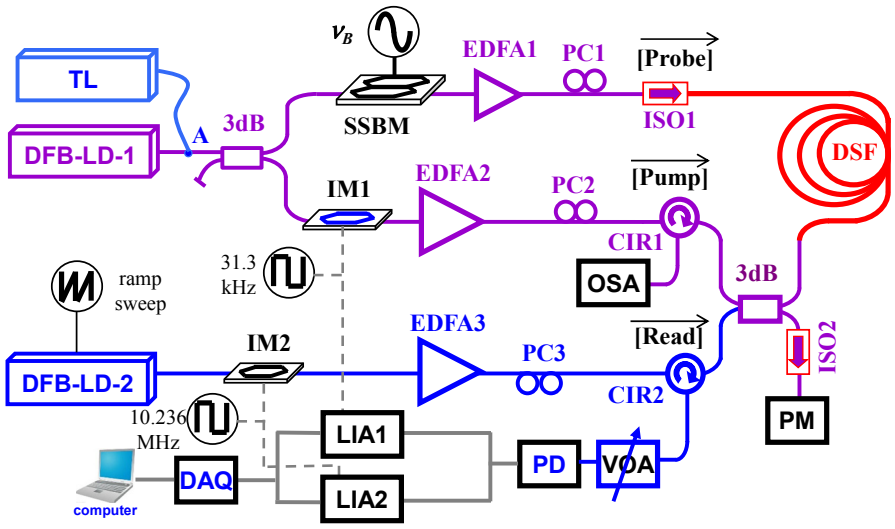

Fig. 2. Experimental setup of characterizing BDG in a DSF.DFB-LD: distributed feedback laser diode; TL: tunable laser; SSBM: single sideband modulator; EDFA: erbium-doped fiber amplifier; PC: polarization controller; ISO: isolator; CIR: circulator; PM: power meter; LIA: lock-in amplifier; IM: intensity modulator; DSF: dispersion-shifted fiber; VOA: variable optical attenuator; PD: photo-detector; DAQ: data acquisition card.

3.2. Qualitative characterization of BDG in DSF

First, the BGS property in the DSF is studied. The DFB-LD-1 is replaced at the "A" point by a tunable laser (TL) with a wide tunable range of 1525-1575 nm. An example of the measured BDG at three different wavelengths is depicted in Fig. 3(a), showing four resonance peaks. The four-peak Lorentz fitting to the experimental data measured at 1551.5 nm is used to estimate the Brillouin parameters of the resonance frequency ($\nu_1^{(i)}$), frequency interval ($\nu_1^{(i)} - \nu_1^{(1)}$), linewidth ($\delta\nu_1^{(i)}$), and relative gain ($g^{(i)}/g^{(1)}$), which are summarized in Table 1. The resonance frequencies are 10.517 GHz, 10.771 GHz, 10.996 GHz, and 11.119 GHz, respectively. When the optical frequency is tuned, the resonance frequencies shifts linearly (see Fig. 3(b)), agreeing with Eq. (5). For instance, the fundamental resonance frequency at 1568.0 nm changes to $\nu_1^{(1)}$ = 10.396 GHz while the neighboring frequency interval keeps almost fixed as 110-250 MHz. The dependence of the first-order and second-order peaks on the optical frequency is plotted in Fig. 3(b). Their acoustic velocities are calculated to be 5679 m/s and 5692 m/s by the least-squares linear fitting and referring to Eq. (5).

Second, an OSA connected with the CIR1 is used to qualitatively characterize the BDG. The wavelengths of the two DFB-LDs are set at1551.5 nm. The pump, probe and read power is 19.0 dBm, −12.5dBm, and 17.5dBm, respectively. The experimental results are summarized in Fig. 4.The pump-probe frequency offset (ν_1) is set to the fundamental resonance frequency of $\nu_1^{(1)}$ = 10.517 GHz by the SSBM. As shown by black curve, the single-sideband suppression ratio of the probe wave can be more than 30dB.When the pump and probe are launched together into the DSF, the probe is amplified by the pump with the gain of 10 dB (from −23 dBm to −13 dBm) via the SBS process. Correspondingly, a strong BDG is generated. If only a read wave is injected into the fiber, a weak backscattered Stokes wave with a peak power of −56 dBm and a high Rayleigh scattering are measured (see gray curve). However, if all pump, probe and read are launched simultaneously, the weak Stokes wave can be extremely enhanced by 50 dB (from −56 dBmto −6 dBm), which is attributed to the pre-excited BDG by the pump-probe SBS process. The absolute reflectivity of the BDG

#189904 - $15.00 USD Received 7 May 2013; revised 10 Jun 2013; accepted 10 Jun 2013; published 13 Jun 2013

can be defined by $R \equiv P_{BDG}/P_{read}$ where P_{BDG} and P_{read} are the BDG reflection power and the read power, respectively [1]. According to Fig. 4, P_{BDG} = 0.20 mW (from −13 dBm to −6 dBm) and P_{read} = 56 mW (17.5 dBm).Consequently, the absolute reflectivity of the BDG is estimated to be R = 0.20/56*100% = 0.36%.

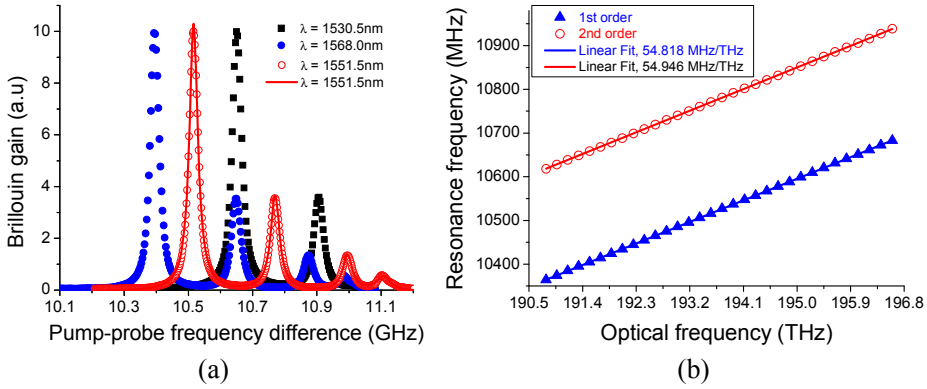

Fig. 3. (a) BGS in DSF measured at three optical wavelengths (or frequencies). The solid curves denote the four-peak Lorenz fitting to the experimental data (symbols). (b) Dependence of the resonance frequencies of the first-order and second-order peaks on the optical frequency. The solid lines correspond to the linear fitting to the experimental data (symbols).

Table 1. Parameters of BGS and BDG in a single-mode DSF characterized at 1551.5 nm

	Parameters	Peak 1	Peak 2	Peak 3	Peak 4
BGS	$\nu_1^{(i)}$ (GHz)	10.517	10.771	10.996	11.119
	$\nu_1^{(i)} - \nu_1^{(1)}$ (MHz)	0	254	479	602
	$\delta\nu_1^{(i)}$ (MHz)	31	34	36	52
	$g^{(i)}/g^{(1)}$	1	0.38	0.07	0.09
BDG	$\Delta f^{(i)}$ (MHz)	0	256	483	611
	$\delta(\Delta f^{(i)})$ (MHz)	48	45	49	89
	ζ_{BDG}	1	0.40	0.17	0.14

3.3. Quantitative characterization of BDG in DSF

To quantitatively characterize the BDG in the DSF, the chopping frequencies to the IM1 and IM2 are set to be inharmonic, i.e., 31.3 kHz and 10.236 MHz, respectively. The pump-probe frequency is also fixed at the fundamental resonance frequency of ν_1 = 10.517 GHz so as to excite the fundamental acoustic mode working as the BDG. The optical wavelengths of the pump and read waves are preset approximately equal to each other at 1551.5 nm. All the optical power is the same as Fig. 4.The measured results by the LIA1 and LIA2 during the detuning of the read wave's optical frequency within a range of ~800 MHz are depicted in Figs. 5(a) and 5(b), respectively.

In Fig. 5(a), the locked signal by the LIA1 under the situations without and with the read wave is compared. If the read wave is turned off, only a constant power is detected since the pump-probe frequency is fixed and the probe wave suffers a constant Brillouin gain from the pump wave. The locked signal by the LIA2 is compared in Fig. 5(b) when the pump wave is turned off or on. It is clear that the signal at the on state of the pump wave is extensively stronger than that at the off state. At the off state, only the SBS interaction between the

#189904 - $15.00 USD Received 7 May 2013; revised 10 Jun 2013; accepted 10 Jun 2013; published 13 Jun 2013

sweeping read wave and the probe wave occurs; while at the on state, a strong pre-excited BDG reflects the read wave efficiently.

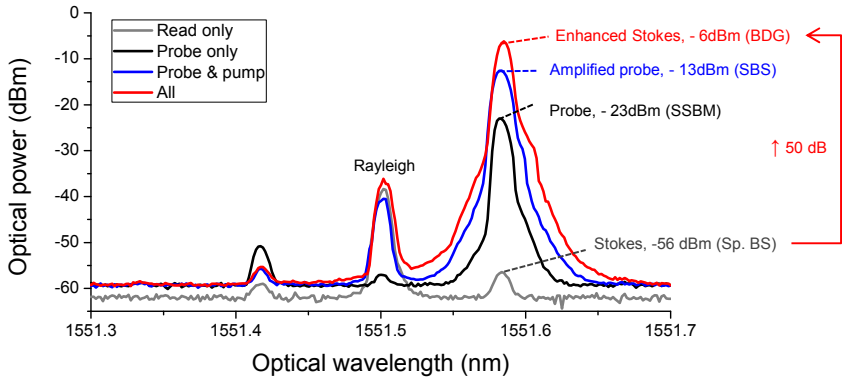

Fig. 4. Qualitative characterization of BDG in a DSF measured by an OSA. The pump, probe, and read powers are 19.0 dBm, −12.5 dBm, and 17.5 dBm, respectively.

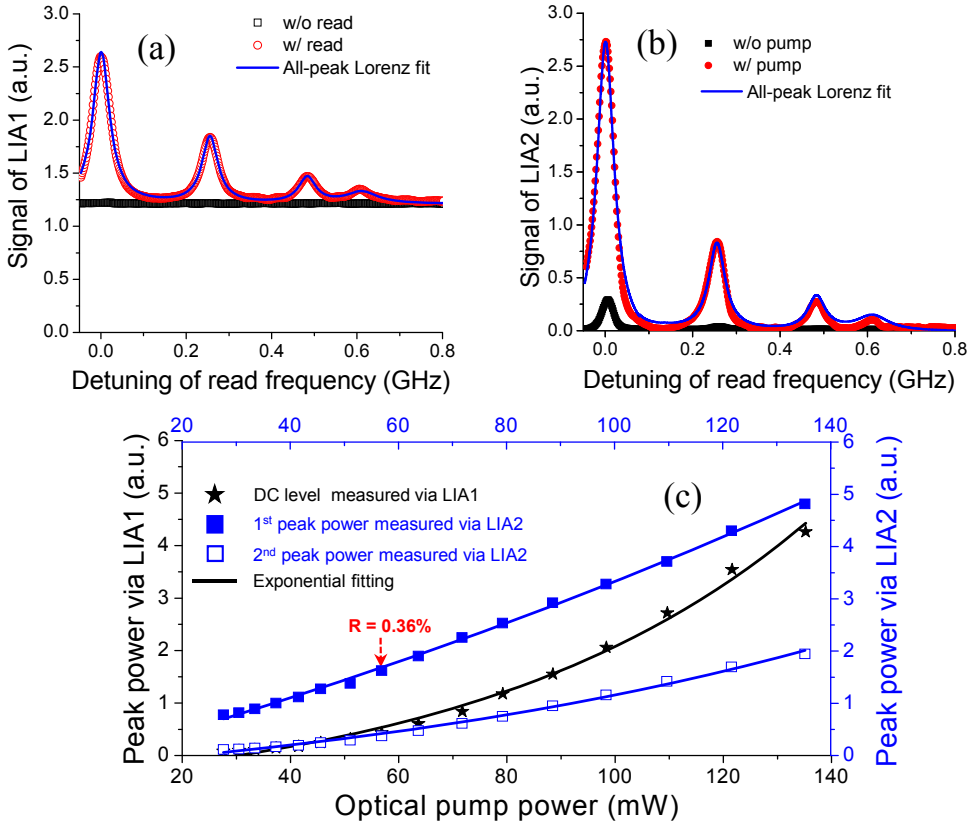

Fig. 5. Quantitative characterization of the BDG reflection measured by the LIA1 (a) and LIA2 (b). The solid curves in (a) and (b) denote the four-peak Lorenz fitting to the experimental data (symbols). (c) The constant Brillouin gain measured by the LIA1 and the peak power of the first-order or second-order peak in the BDG reflection measured by the LIA2 as functions of the optical pump power. The absolute reflectivity of BDG measured by OSA is also shown.

Clearly shown in Fig. 5(a) and Fig. 5(b), four resonance peaks appear in the BDG reflection when all pump, probe and read waves are launched into the DSF. The four-peak

#189904 - $15.00 USD Received 7 May 2013; revised 10 Jun 2013; accepted 10 Jun 2013; published 13 Jun 2013

Lorentz fitting is taken again to estimate the parameters of the BDG reflection, including the frequency difference ($\Delta f^{(i)}$), the bandwidth $\delta\Delta f^{(i)}$, and the fact (ζ_{BDG}) determining the energy coupling efficiency. The results are also summarized in Table 1. The frequency differences are approximately equal to the frequency interval of the resonance frequencies of the BGS, which matches the theoretical analysis given in Eq. (8). The ζ_{BDG} and $\delta(\Delta f^{(i)})$ of four peaks are also comparable to the corresponding parameters of the BGS, which agree with the estimation of Eq. (9).

Figure 5(c) illustrates the dependence of the BDG reflection on the pump power. First, the constant gain measured by the LIA1 increases nonlinearly with the pump power, which is due to the exponential Brilloin gain of the SBS interaction [10]. Second, both the first-order and second-order peaks in the BDG reflection are also exponentially dependent on the pump power. It confirms that the nature of the BDG generation and reflection should be attributed to the SBS process. Referred to the absolute BDG reflectivity characterized at 17.5-dBm pump power [marked in Fig. 5(c)], the one at 21 dBm can be as high as 1.26%.

4. Conclusion

We have proposed and demonstrated a new method to generate the BDG based on multiple acoustic modes in a single-mode DSF. The generation of the BDG is realized by two coherent optical waves with a precise frequency offset equal to the BFS (i.e., the fundamental acoustic frequency); the BDG reflection of the read wave occurs in multiple separate frequencies corresponding to multiple acoustic modes existing in the single-mode DSF. The theoretical analysis matches well the experimental observation. It is expectable that an optimization of the fiber structure [18] will lead to the enhancement of the reflection efficiency when the higher-order acoustic mode is utilized. This new BDG generation with frequency-maintained or frequency-shifted property will attract interest in potential applications to two-end-access and one-end-access Brillouin-based fiber-optic sensing [1–7, 14, 19], tunable delay line [8], photonic microwave filter [9], and all-optical signal storage [20, 21].

Acknowledgments

This work is supported by the National “973” Program of China (No. 2011CB301700), the National Natural Science Foundation of China (Grant No. 61007052, 61127016, 61107041), the International Cooperation Project from the Ministry of Science and Technology of China (Grant No. 2011FDA11780), Shanghai Pujiang Program (Grant No. 12PJ1405600), Shanghai Excellent Academic Leader Program (Grant No. 12XD1406400), and the “SMC Young Star” Scientist Program of Shanghai Jiao Tong University.

#189904 - $15.00 USD Received 7 May 2013; revised 10 Jun 2013; accepted 10 Jun 2013; published 13 Jun 2013